Scientific report; 98 - 05

KNMI

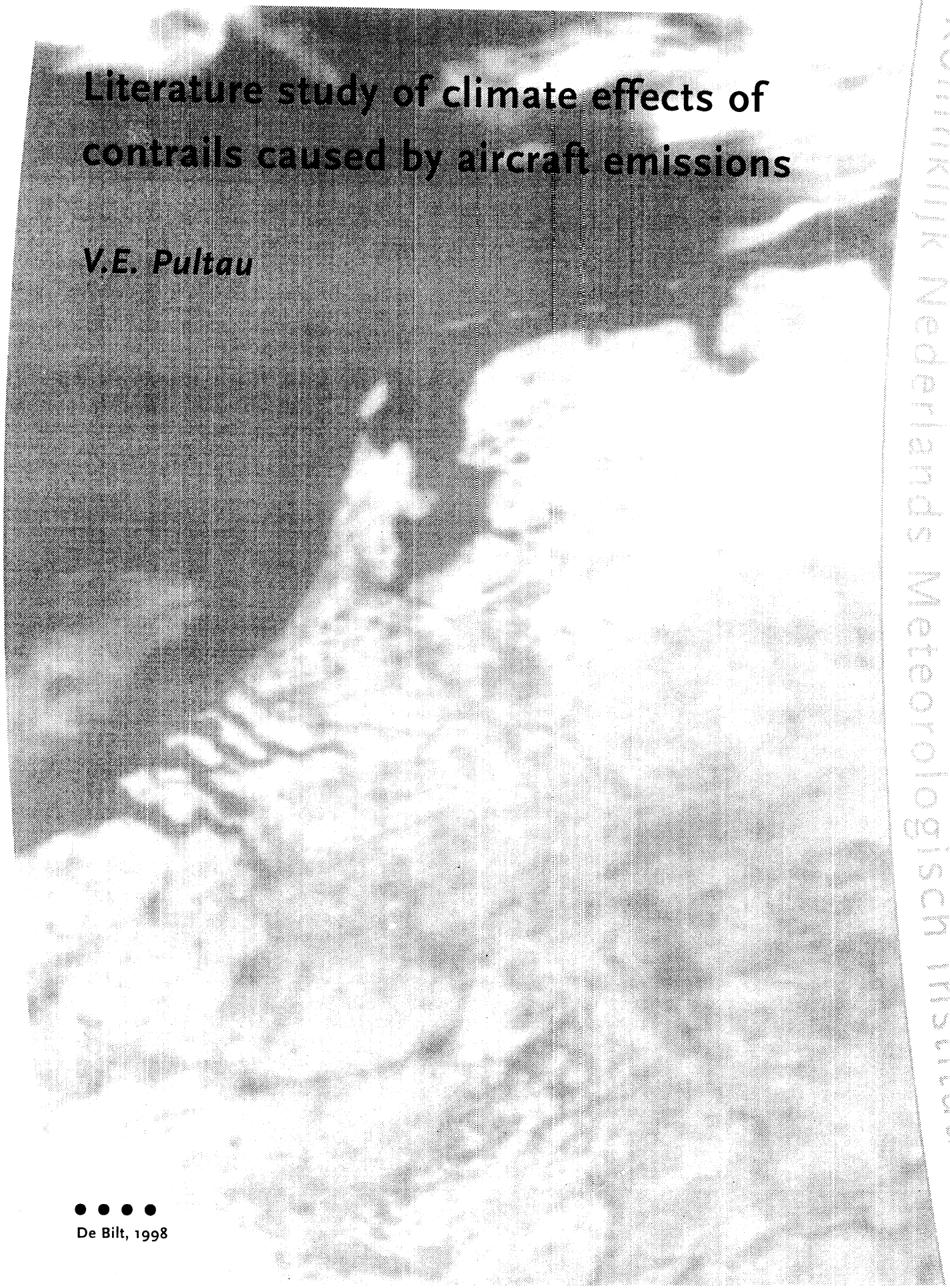

Literature study of climate effects of contrails caused by aircraft emissions

V.E. Pultau

Koninklijk Nederlands Meteorologisch Instituut

De Bilt, 1998

Scientific report = wetenschappelijk rapport; WR 98-05

De Bilt, 1998

PO Box 201
3730 AE De Bilt
Wilhelminalaan 10
De Bilt
The Netherlands
Telephone +31(0)30-220 69 11
Telefax +31(0)30-221 04 07

Author: V.E. Pultau

UDC: 551.510.42
551.576.11
656.7

ISSN: 0169-1561

ISBN: 90-369-2151-1

Scientific report; WR 98-05

Literature study of climate effects of contrails caused by aircraft emissions

V.E. Pultau

De Bilt, 1998

Introduction

On demand of EUROCONTROL, a study of the most recent literature concerning contrails was performed. Attention was paid to the latest research findings concerning the formation (section 1), the lifetime (section 2), frequency (section 3), the microphysical properties (section 4) and the radiative forcing (section 5) of contrails and their climate effects.

Contrails form when saturation with respect to water is temporarily reached in the plume and they persist in ice supersaturated air masses. The ambient temperature necessary for contrail formation can be predicted accurately.
Contrail particles consist of ice crystals. Young persistent contrails are composed of more, but smaller ice crystals than typical cirrus. Persistent contrails develop towards cirrus clouds in the course of time.
The average contrail coverage exhibits a value around 0.5% over Europe. The mean global contrail cover is estimated to be of order of 0.1%.
The net radiation effect of contrails is believed to enhance warming of the troposphere on average.

1. Contrail formation

Contrails formed by jet aircraft in the upper troposphere are an artificial form of cirrus cloud and can often not be distinguished from natural cirrus clouds. Contrails may even be transferred into cirrus clouds after a certain time. Natural cirrus as well as contrails contain ice crystals.
Contrails tend to form in the vicinity of the tropopause. For example: the approximate elevation of the contrails observed by Duda *et al.*[41]. is 9.2 km. Sassen *et al.*[42] observed a variety of contrails with uniform heights between 11.5-12.5 km above MSL. The great majority of the Salt Lake City contrails observed by Sassen[7], occur between 9.0 to 13 km above sea level.
Contrails are frequently visible at distances as close as 25-35 m behind the aircraft engines[5], implying that the ice particles form and grow large enough to become visible within the first tenths of a second of plume age. Contrails can grow up to several kilometres wide but are only a few hundred meters thick (200 to 400 m). This is due to the vertical stability of the atmosphere at these heights.

The formation of contrails is due to the increase in relative humidity (RH) that occurs during the isobaric mixing of the hot and humid exhaust gases with the colder and less

humid ambient air. The RH must reach 100% in the young plume behind the aircraft for contrail formation to occur[5, 33].

One can, by thermodynamic means, derive a relationship that yields the maximum ambient temperature below which a contrail forms (**threshold condition**). In order to form a contrail, the ambient air must be cold, typically colder than 233K, but the precise threshold value depends on -pressure or altitude

-ambient humidity

-the amounts of combustion heat and water vapor (EI_{H2O} [1])released from the aircraft and

-overall aircraft propulsion efficiency, η [2]

The Schmidt-Appleman[1] criterion (supersaturation with respect to water reached during the mixing of the exhaust gas with the ambient air) has proven to be very successful at predicting the occurrence of contrails (see Appendix A).

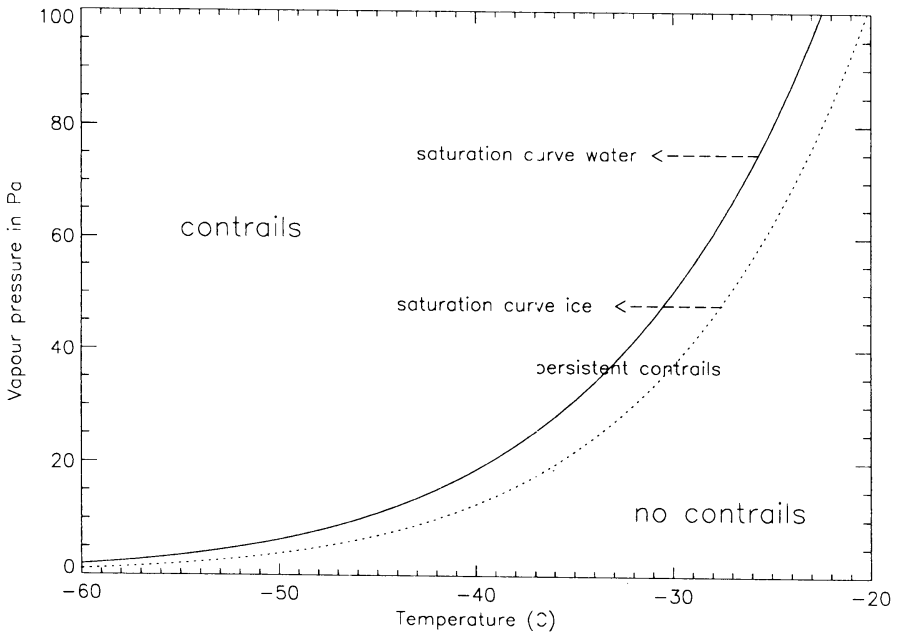

Figure 1: Water vapour partial pressure versus temperature with saturation for liquid water (full curve) and ice (dashed).

[1] EI_{H2O}=Emission index of water (1.25 kg H_2O per kg fuel burnt)

[2] η=fraction of combustion heat that is used up to propel the aircraft and thus is not available to heat the plume. It can be computed from engine and aircraft properties; the mean overall propulsion efficiency of subsonic aircraft at cruise was close to 0.22 in the 1950's, near 0.37 for modern engines in the early 1990's and may reach 0.5 for new engines to be built by 2010.

The ATTAS experiment by Busen and Schumann[5] as well as flow field calculations of Kärcher[48] show that contrails should become visible below the water saturation threshold, but above ice saturation threshold, thus extending the classical formation criterium discussed by Appleman[1] to higher threshold temperatures (for a given ambient relative humidity and pressure).

The modification of the Appleman criterion by Schumann[2] -to account for engine efficiency- was needed in order to explain discrepancies found between observed and computed threshold conditions. The kinetic energy of the young exhaust plumes has however only a minor effect on the threshold conditions. The inaccuracy of radiosonde humidity measurements (operational humidity data tend to underestimate the humidity in the upper troposphere) and the spatial separation between the contrails and the radiosoundings offer an interpretation of the ATTAS experiment.

Schumann *et al.*[29] reported in situ measurements of humidity and temperature at contrail onset times. These results were in agreement with the theoretical predictions of threshold temperatures, assuming liquid saturation is required for contrail formation. SUCCESS[3] measurements reported by Jensen *et al.*[30] showed that contrail onset temperatures for contrail formation are 0-2 K below the liquid-saturation threshold temperatures, implying that saturation with respect to liquid water must be reached at some point in the plume evolution.

Contrail particles consist of **ice** particles. Ice can form through several processes including

-the freezing of water droplets (*homomolecular-homogeneous* nucleation)

-the freezing of liquid aerosols (H_2SO_4/H_2O) droplets (*heteromolecular-homogeneous* nucleation)

-vapor phase deposition of ice onto solid aerosols e.g. soot (*homomolecular-heteromolecular heterogeneous* nucleation).

These nucleation processes are all strongly depending on temperature and relative humidity and the type of cloud condensation nuclei.

In contrail particle formation, heterogeneous freezing processes involving soot compete with the homogeneous freezing of volatile plume particles. Present observations do not conclude unambiguously which mechanism causes freezing.

[3] SUCCESS=Subsonic aircraft: Contrail and Cloud Effects Special Study

- Due to competition with the other processes, homomolecular-homogeneous nucleation of water droplets is very unlikely to take place in the wake.
- Soot is expected to play an important role in the formation of visible ice contrails under threshold formation conditions. Fresh soot particles do not act as efficient as ice deposition nuclei; consistent with the absence of contrails at temperatures above the liquid water saturation threshold. A large fraction of these combustion aerosols must be activated (e.g. by acquiring a liquid H_2SO_4/H_2O coating) and freeze heterogeneously at temperatures below about 230-235 K. Contrails observed near the threshold formation conditions are thought to result from freezing of ice within water-activated soot particles.
- Using a trajectory box model, Kärcher *et al.*[3,4] could show that homogeneous freezing of H_2SO_4/H_2O droplets generated in situ do not lead to visible contrail formation when temperatures approach the Appleman threshold condition, because freezing time scales are too long and predicted ice particle concentrations are too low.

  This ice formation process should show a strong dependence on the sulfur content, which was not observed by Busen and Schumann[5].
- However, well below threshold formation conditions, at temperatures below 215K, when the plume becomes supersaturated with respect to water, homogeneous freezing could in principle, compete with heterogeneous processes.
- Simulations also suggest that contrails would also form without soot and sulfur emissions by activation and freezing of background particles[59].

2. Lifetime

2.1 Persistence

The lifetime of contrails have been found to be largely controlled by humidity and temperature of the air surrounding the contrail. Boin and Levkov[13] found a (nearly) exponential increase of the contrail lifetime with increasing relative humidity.
Persistent contrails occur in ambient air which is supersaturated with respect to ice and not saturated with respect to the water phase[28]. Without ambient ice-saturation, contrail ice crystals evaporate on the time scale of seconds to minutes, unless the particles are coated with other species such as HNO_3[(50)].
For all the cases considered in the study of Jensen and Toon[30] for which the contrails persisted longer than a few minutes, the ambient air was substantially supersaturated with respect to ice.

Atmospheric conditions suitable for contrail persistence are widespread and vary with latitude representing about 10 to 20% of the area over mid Europe (Mannstein *et al.*[44]) and parts of the USA (Travis and Changnon[45]). Hence as air traffic increases, contrail coverage is expected to increase up to a limit of 10 to 20% in these areas.
Based on ECMWF analysis for years 1990-1994, Brockhagen[46] found that up to 6% of the area of the globe pass the criteria for persistent contrails.

Persistent linear contrails can evolve over a matter of hours to form extensive cirrus clouds. The presence of contrails is thought to initiate the formation of cirrus that would otherwise not have formed. An increase in contrail frequency is expected to increase the occurrence and coverage of cirrus clouds.
Recently, cirrus cloud cover trends have been derived. The cirrus cloud cover data were averaged on a seasonal basis for the USA, North Atlantic, Europe, Western Asia and the North Pacific (referred to as ATR, air traffic regions) for two separate periods, 1971-1981 and 1982-1992. Significant decadal increases in cirrus cover occurred in most ATRs in the first period with the largest annual values found in the USA (3%), Western Asia (1.6%) and the North Pacific (1.7%). No significant trends were found over Europe in either period. On average over all ATRs, the cirrus increase in 1971-1981 amounts to 1.5% cover per decade, compared to an average of 0.1% for the rest of the globe. From 1982 to 1991, cirrus cover decreased over all areas except over the USA and the North Pacific where it increased by 1.2% and 2.2%, respectively.

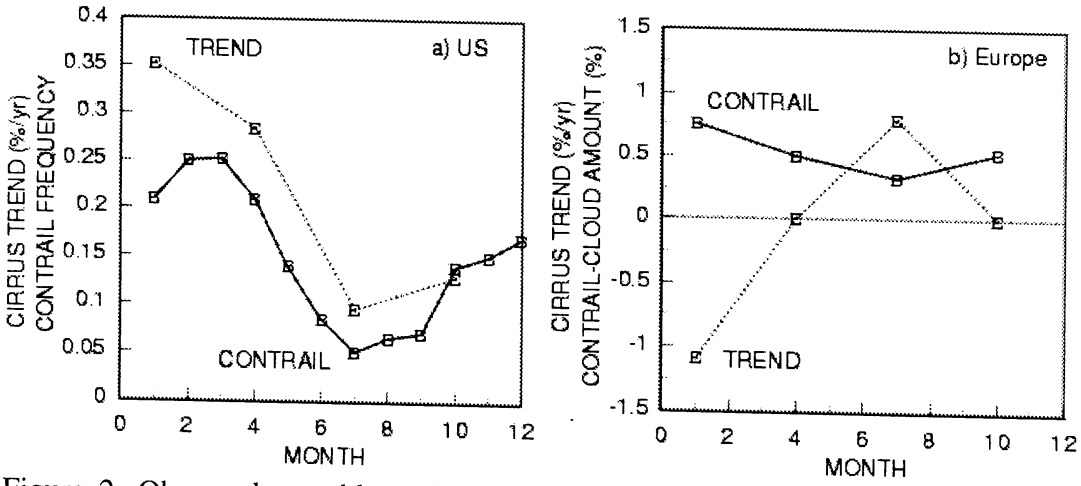

Figure 2: Observed monthly variation of contrail occurrence frequency during one year for the USA (a) and Europe (b), solid squares, and seasonal mean trends of observed fractional cirrus cover (open circles) in the time period 1971 to 1992 for the USA and 1971-1982 for Europe

In Figure 2, the seasonal cycle of the averaged trends in cirrus cover over the USA and Europe are compared to the seasonal trends of contrail occurrence or cover, respectively. The contrail trends are derived from one year of data from USA surface stations (Minnis *et al.*[49]) and from satellite data over mid-Europe (Mannstein *et al.*[44]).

For the USA, the trend of cirrus cover is similar to the cycle of contrail occurrence (Figure 2a), suggesting that cirrus changes are related to contrail occurrence. For Europe, the trends do not resemble the seasonal cycle of contrail cover (Figure 2b) and, therefore, are inconclusive regarding the role of aircraft.

A few investigations show contrails with significant precipitation, but sedimentation of ice crystals only becomes important when contrails are formed and persist in strongly supersaturated air[51, 52, 53].

2.2 Contrail growth

From surface lidar observations of exhaust plumes aged between 1 minute and 1 hour Freudenthaler *et al.*[7] deduced that, in agreement with model calculations of contrail spreading and observations of Sassen[7], a much faster horizontal than vertical growth of the contrail. The impact of shear motion on the evolution is clearly visible: turbulence created by the aircraft vortices are sufficient to explain the spreading rates in younger contrails but ambient shear soon dominates further spread (e.g. Gertz *et al.*[10]).

3. Frequency

At present there are no data on the actual coverage of the earth by contrails, except for certain selected regions. Several authors have estimated the observational frequency of occurrence of contrails[4] and the fraction of the sky covered by contrails directly or indirectly from the surface and satellite observations.

- Schumann and Wendling[8] found that contrails, on average, covered 0.4% of **Central Europe** (derived from AVHRR images)
- A study by Bakan *et al.*[9] reveals an average contrail cloudiness of about 0.5% over the period 1979 to 1982 for the region covering **Europe** and **Eastern Atlantic Ocean** (30°W to 30°E, 35°N to 75°N). They found a distinct seasonal cycle with a

[4] % time they occur

southward displacement of the contrail maximum during winter. Maximum cloudiness of 2% occurred during summer centred along the North Atlantic air routes.

- **Day/night** contrail cover ratios of about 2 (Bakan *et al.*[9]) over **Europe** and the eastern part of the **North Atlantic**, or 3 over **Mid-Europe** (Mannstein[11]) have been deduced, consistent with a global mean noon/midnight traffic ratio of 2.8 (Schmitt and Brunner[12]).
- The contrails identified by Mannstein[11] over **Central Europe** are not uniformly distributed, but lie along air traffic corridors and reveal a coverage of at least 0.5%. The maximum coverage occurred during spring and winter.
- Contrails are also common over much of the **USA**. Data, available from surface based observations at 19 locations across the continental USA for every hour in the period 1993-1994, indicate that contrail frequency peaks around February/March, with a minimum during July. The annual mean persistent contrail frequency (not the cover) for the 19 sites was 12%; extended to the remainder of the country, the mean annual contrail frequency is estimated to be 9% (Minnis *et al.*[34]). A relationship between fuel usage and contrail frequency could be obtained; such a relationship suggests that the area of the Earth covered by contrails currently is limited by the number of aircraft flights rather than the atmospheric conditions needed for contrails to form.
- Sassen[7] found, from sky photographs taken between 1986-1996 over **Salt Lake City** (Utah), a seasonal cycle in contrail coverage with a maximum in fall and winter and a minimum in July.
- Both Sassen[7] and Minnis *et al.*[34] found that contrails occur together with natural cirrus in approximately 80% of the observations.
- Based on temperature, humidity and traffic data, and 0.5% contrail cover over Europe, the **global** contrail cover is estimated to be of order 0.1%

Another approach to quantify the area covered by contrails is to identify the part of the atmosphere where contrails may form, and use the amount of fuel burned in these regions to estimate the contrail coverage.
Sausen *et al.*[35] used ECMWF reanalysis data, the Appleman-Schmidt criterion and a subgrid parameterization of cirrus formation conditions to estimate the frequency of air masses that are cold and humid enough to carry contrails. This potential contrail cover is found to be largest in the upper troposphere (global mean value 16% cover), in particular in the tropics. The potential contrail cover over Europe is 12%, which compares well with the estimate given by Mannstein *et al.*[43].

Ground observers report a mean cirrus cover of 13% over oceans and 23% over land; satellite data identify larger cloud cover of about 40% by subvisible ($\tau_{0.55_{\mu m}}$<0.03) and semitransparent (τ<6) cirrus clouds (τ=optical thickness, section 4).

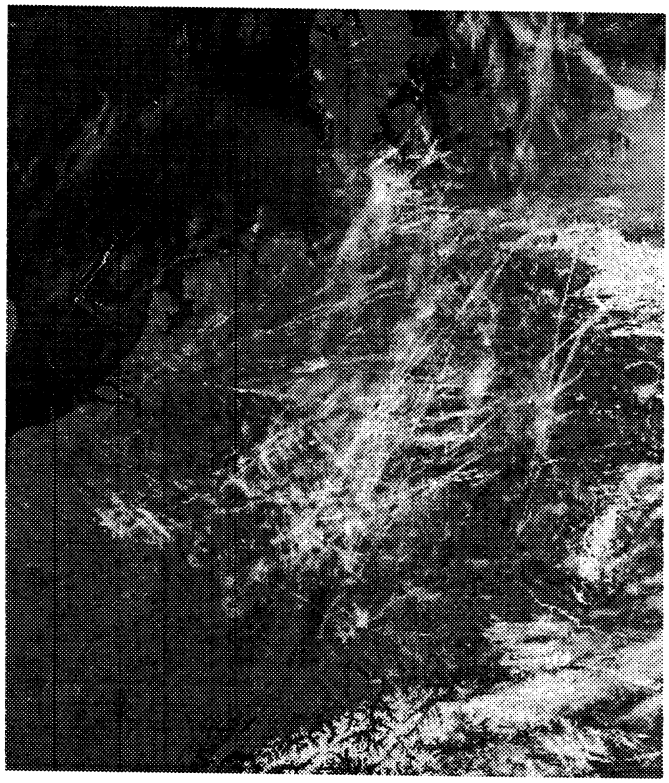

Figure 3: Contrails over central Europe on 0943 UTC 4 May, based on NOAA12 AVHRR satellite data (Mannstein [11])

4. Microphysical properties

Crystal sizes in young persistent contrails (up to ~1hr) are smaller (**mean radius of 5 to 15 μm**) than in typical cirrus clouds (15 μm to 50μm) but grow as the contrail ages and may approach the size of natural cirrus particles within a time scale of order one hour.

Betancor Gothe and Graβl[20] showed that the longwave characteristics of contrails only match satellite observations for crystal sizes around 4 to 6 μm. Satellite data revealed an effective radius of 4.5 μm for contrails versus 27 μm for cirrus clouds[21] (under the assumption of spherical particles). In situ measurements of ice spectra revealed effective radii of 15 to 18 μm for contrails versus 24 to 30 μm for natural cirrus (Gayet[17]).

Strong depolarisation is found in contrails older than a few minutes, indicating nonspherical particles [6, 22].

A realistic particle size spectrum is given by Strauss *et al.*[23] which covers the range from 2 to 2000 μm (cirrus) and from 2 to 200 μm (contrails, volume-mean particle radius 8.2 μm)

Duda *et al.*[41] inferred estimates of cloud particle size from multi-spectral observations. The particles in a newly formed contrail were generally smaller (effective radii on the order of 10 μm) than those in an older contrail whose microphysics resembled those of the surrounding cirrus.

Sassen and Hsueh[42] studied a variety of contrails ranging from a newly formed to persistent contrails. Brilliant corona displays are often found as persisting contrails drift under the sun, indicating particles in the 10-30 μm range.

Liou *et al.*[40] analysed four ice crystal distributions for contrail cirrus. Based on the *in situ* observed data, they propose an ice crystal shape model for contrails consisting of 50% bullet rosettes, 30% hollow columns and 20% plates with sizes ranging from 1 to 90 μm. The mean effective sizes for the 4 observed ice crystal size distributions (using the above combination; D_e defined in terms of maximum dimension) are 4.9, 9.8, 15.9 and 13.3 μm.

The measurements by Lawson *et al.* [52] show that after 40 minutes the size distributions of particles within the core of the contrail differ from those on the periphery. The core contained mostly small ice particles (1 to 20 μm) which appeared spheroidal in shape, while in the periphery, ice particles as large as 300-500μm were observed. Particle shapes in the periphery included unresolved spherical, irregular, columnar and bullet rosettes. Ice crystals larger than about 200 μm were typically bullet rosettes.

The ice crystals in the contrail (after about 1 minute growing time) collected by Goodman *et al.*[58] were predominantly hexagonal plates (75%), columns (20%) and few triagonal plates (<5%).

The optical thickness τ of contrail clouds varies widely. Very thick contrails (~700m) have been found at low altitude with optical thickness exceeding 0.8[8], however most contrails observed within an hour of formation over a.o. Germany[14,15], Oklahoma[16], and Salt Lake City[7] exhibit an optical thickness below 0.5.

Minnis *et al.*[32] describe satellite observations of three cases (2 distinctive and one set of contrails), the visible wavelength optical thickness ranged from 0.2 to 0.5.

The mean optical thickness retrieved in the contrail observed by Duda *et al.*[41] was roughly 0.35, while the cirrus optical thickness ranged from near zero to over 1.5.

The number density of ice crystals in contrails is in the order of 10 to 100 cm^{-3}, which is much larger than in cirrus clouds[53].

Ice water content (IWC) values in aged contrails vary between 0.7 and 2.1 mg m^{-3} [7], 2 to 18 mg m^{-3} [17] and 0.7 to 6 mg m^{-3} [18] consistent with numerical studies [19].
It appears likely that the IWC of contrails depend on ambient temperature, because the amount of water available between liquid and ice saturation increases with temperature T for T less than -12°C.

5. Radiative forcing of contrails: previous studies

Aircraft emissions may possibly have the strongest impact on climate through changes in cloudiness and their impact on the Earth's radiative budget. Both surface and upper tropospheric temperatures may change as a result. Modifications may occur directly due to additional contrail clouds or indirectly due to changed cirrus cloud properties. Aviation-induced aerosol may impact cirrus clouds indirectly through changes in the nucleating properties and the number and size distribution of cloud particles. Several studies have addressed the direct impact of contrails; the indirect effect of contrails has not yet been investigated in detail.

The ultimate energy source for all weather and climate is radiation from the sun (called **solar** or **short-wave radiation**). Averaged globally and annually, about a third of the incoming solar radiation is reflected back to space. Of the remainder, most is absorbed by the earth (some by the atmosphere). The solar radiation absorbed by the earth's surface and atmosphere is balanced at the top of the atmosphere by outgoing radiation radiation at infrared wavelengths (**longwave radiation**). Some of the outgoing IR radiation is trapped by the naturally occurring greenhouse gasses (H_2O-vapor, CO_2, O_3, CH_4 and N_2O and by clouds. This is the *natural greenhouse effect*. In a unpertubated state, the net incoming solar radiation at the top of the atmosphere must be balanced by net outgoing infrared radiation. Additional greenhouse gases or clouds can lead to an enhanced greenhouse effect.
Radiative forcing is defined as the net radiative flux change at the tropopause calculated in response to some perturbation, such as a change in cloud cover. A positive (negative) net flux change represents an energy gain (loss) and hence a net heating (cooling) of the Earth-troposphere system.

The longwave (LW) radiative forcing is greatest when the clear-sky radiative flux to space is large, (i.e. larger over warm than over cool surfaces, larger in a dry than in a

humid atmosphere) and when the cloud emissivity is large (the emissivity increases with ice water path (IWP) [5]).

The shortwave (SW) radiative flux is mainly determined by the solar zenith angle and the cloud optical thickness (which increases with the IWP)
For fixed IWP, clouds containing smaller particles have larger optical thickness and exhibit larger solar albedo; aspherical particles cause a larger albedo then the spherical ones.
The SW forcing is negative when the cloud causes an increase of the system albedo. In general, SW forcing has greater magnitude over dark surfaces than over bright surfaces.

The imbalance between the albedo (shortwave radiative forcing) and greenhouse effects (longwave radiative forcing), which determines the sign of the climatic impact is mainly a function of cloud particle size. Clouds containing relatively small particles tend toward increased solar reflectances versus the more active trapping of terrestrial infrared radiation when larger particles dominate.The magnitude and possibly even the sign of the daily mean net radiative forcing of contrails depends on the diurnal cycle of contrail cover; a large day to night ratio of contrail cover reduces the net radiative forcing.

The minimum set of parameters necessary to assess the radiative impact of contrails consist of the vertical temperature and humidity profile, surface temperature and its diurnal cycle, the vertical altitude and geometrical thickness of the contrails, the cloud cover, the IWC or the number of ice particles, the particle size and shape spectra, the surface scattering properties, the latitude, time of year and the daily ratio between daytime and night-time contrail or air-traffic occurrence.

Hereafter follows a review of previous studies concerning the direct effects by scattering and absorbing solar and longwave radiation by contrails.

- The change in radiative fluxes, assuming a 0.5% increase in cloud cover just below the tropopause and considering IWP-values of 4 to 50 gm^{-2} and effective crystal radius of 4 to 100μm, has been computed by Fortuin *et al.*[24]. Their broadband radiative transfer calculations estimate a radiative forcing by contrails in the North Atlantic Flight Corridor in the range -0.2 to 0.3 Wm^{-2} in summer and 0.0 to 0.3 Wm^{-2} in winter.

[5] IWP=the integral of the cloud ice water content of the cloud over its geometrical thickness

• Strauss *et al.*[23] modelled a 0.03 Wm^{-2} radiative flux change at the tropopause and a surface temperature increase over Europe of ~0.05K for a 0.5% current contrail cloud cover.

• Using a 2-D radiative convective model a 1K increase in surface temperature was found over most of the Northern Hemisphere for an additional cirrus cover of 5% (Liou *et al.*[37]).

• Ponater *et al.*[38] simulated the potential effects of contrails on global climate using a GCM. The induced temperature change is significant for a 5% additional cirrus cloud cover in the main traffic zones, indicating the importance of contrails.

• Meerkötter *et al.*[28] computed the radiative forcing due to an additional cloud cover by contrails for a set of atmospheric conditions using established radiation transfer models[54, 55, 23, 56, 57]. The contrails cause negative SW and positive LW flux changes. The net forcing is positive in all cases considered, suggesting that contrail heating generally prevails over cooling in the atmosphere/surface systems.

The sensitivities of net contrail forcing to various parameters of a contrail in a midlatitude summer continental reference case were computed.As a result of this sensitivity study, contrail heating becomes more effective with increasing

-surface temperature

-surface albedo

-IWC

For the same IWC, contrails with small ice particles are more effective in radiative forcing than contrails with large particles.

As a whole, the TOA[6] radiative forcing is only weakly sensitive to key parameters except for the optical thickness and the contrail cover, with which the forcing scales about linearly.

The global distribution of radiative forcing is computed using the two-stream model of Liou, the contrail cover as derived by Sausen *et al.*[35]. The global mean SW forcing is negative, the LW is positive and the net is also positive: 0.0081 Wm^{-2}, 0.0165 Wm^{-2} and 0.0203 Wm^{-2} at TOA in the global mean for a solar optical thickness of 0.1, 0.3 and 0.5 respectively.

The global distribution of the net forcing at TOA for $\tau = 0.3$ is large in regions of busy air traffic, with maximum values of 0.71 Wm^{-2} over north-east France and 0.58 Wm^{-2} near New York.

• Sassen *et al.*[7] measured a strong reduction (>50 Wm^{-2}) in the solar radiation received at the surface when a contrail passed over the measurement site while the

[6] TOA=Top Of Atmosphere

IR data did not show a noticeable change. The results were interpreted as a cooling effect.

- Kuhn[26] measured 10 to 20% reduction of net downward radiation just below a ~500m thick contrails with about 7% reduction (computed) of net fluxes reaching the surface. This reduction could cause a 5K cooling during the day if the contrail would persist.
- Wendling *et al.*[27] find a 30 Wm^{-2} reduction of net downward radiation below a contrail definitively demonstrating cooling.

It is possible that a strong localised initial cooling of a young contrail evolves into a more widespread heating after some time when the contrail looses its identity. The temporal evolution of a single contrail property probably strongly affects its radiative forcing.

During night, contrails cause heating of the surface, thereby causing higher minimum temperatures and reducing the diurnal temperature range, DTR (difference between daily maximum and minimum temperature). The change in DTR was estimated to possibly reach 1 to 5 K if the contrail cover would persist the whole day [26].

6. Summary

- Contrails form within a short distance behind the aircraft in the expanding plume where supersaturation with respect to liquid water is reached. The threshold temperature for contrail formation can be predicted accurately at a given flight level.
- Contrails persist in ice-supersaturated air masses. Atmospheric conditions suitable for contrail persistence vary with latitude and are estimated to represent about 10 to 20% of the Earth's area at mid-latitudes.
- Ice crystals in young (up to ~1 hour) persistent contrails are smaller (mean radius of 5 to 15 μm) than in typical cirrus clouds.
- The largest contrail cover occurs over the USA, Europe, the North Atlantic and Southeast Asia. Over Europe the annual mean noontime cover by line-shaped contrails amounts to at least 0.5% and one third of this value at night. The mean global contrail cover is estimated to be of order of 0.1%.
- Persistent contrails can evolve over a matter of hours to form extensive cirrus clouds.

The presence of contrails is thought to form cirrus clouds that would otherwise not have formed.

• Contrails cause a local cooling of the surface in the shadow of thick contrails and reduce solar heating of the surface during the day and radiative cooling of the surface during the night, thereby reducing the daily temperature range (order of 1K).
Contrails cause a heating of the troposphere (in particular over warm and bright surfaces). The heating is maximum in the upper troposphere below contrails.
The present estimate is a heating of the tropopause of **0.02 ±0.01 Wm^{-2}** for global contrail cover of 0.1%, with regional maximum values up to 0.7 Wm^{-2} over parts of Europe and the USA

Acknowledgements: Thanks to M. Van Weele, P. Fortuin, P. van Velthoven and H. Kelder for comments and suggestions.

Appendix A

Comparison with radiative forcing through other factors, like carbondioxide, methane, nitrous oxide, halocarbons and ozone[47].

Component	Change	Forcing
CO_2	280 to 356 ppmv [a]	1.56 Wm^{-2}
N_2O	275 to 310 ppbv [a]	0.1 Wm^{-2}
CH_4	0.7 to 1.7 ppmv [a]	0.5 Wm^{-2}
halocarbons, including CFC-11, 12, 13, 113, 114, 115, methylchloroform and carbontetrachloride	observed concentrations	0.3 Wm^{-2}
HCFC's and HFC's	observed concentrations	0.05 Wm^{-2}
contrails	annual and daily mean for global contrail cover of 0.1%	0.02 Wm^{-2}

a: increase since pre-industrial time

Appendix B: Schumann-Schmidt-Appleman criterion:

G is the ratio of rates of change of vapour pressure and temperature in an expanding aircraft exhaust plume

$$G = \frac{EI_{H_2O}\, c_p\, p}{\varepsilon Q(1-\eta)}$$

p = pressure
c_p=specific heat at constant pressure
EI_{H2O}=emission index of water (1.25 kg per kg fuel burnt)
ε = 0.622 is ratio of molecular masses of water and air
Q = 43 MJ/kg fuel is the specific combustion heat of kerosene
η = propulsion efficiency of a jet engine

T_{LM} is (for a given G) the maximum temperature at which contrails can form and can be approximated by (Schumann [2]):

$$T_{LM} = -46.46 + 9.43\ln(G - 0.053) + 0.720[\ln(G - 0.053)]^2 \quad \text{(eq.1)}$$

similarly, T_{IM} is approximated by

$$T_{IM} = -43.36 + 9.08\ln(G - 0.02) + 0.49[\ln(G - 0.02)]^2 \quad \text{(eq.2)}$$

where the temperature is in °C and G is in Pa/K

The threshold temperatures T_{LC} and T_{IC} follow from

$$T_{LC} = T_{LM} - [e_L(T_{LM}) - Ue_L(T_{LC})]/G, \quad \text{(eq.3)}$$

$$T_{IC} = T_{IM} - [e_I(T_{IM}) - Ue_I(T_{IC})]/G \quad \text{(eq.4)}$$

where e_L and e_I = saturation pressures of liquid water and ice resp.

For U=0 and U=1, T_{LC} and T_{IC} follow explicitly from eq.3 and eq.4. Otherwise, approximate values are obtained from a Taylor expansion around point LM giving:

$$T_{LC} = T_{LM} - x, \qquad x = -A + \left(A^2 + 2B\right)^{1/2}$$

with

$$A = \frac{(1-U)G}{U^2 e''_L(T_{LM})}, \qquad B = \frac{e_L(T_{LM}) - e_E}{U^2 e''_L(T_{LM})}, \qquad e_E = Ue_L(T_{LM})$$

and analogous equations for T_{IC}.

The saturation pressures for liquid and ice saturation (in the temperature range $173.15 \le T \le 373.15$ K and $173.15 \le T \le 273.16$ K resp.) can be computed from relations as given by Sonntag[39]:

$$\ln e_w(T) = -6096.9385T^{-1} + 16.635794 - 2.711193\times10^{-2}\,T + 1.673952\times10^{-5}\,T^2 + 2.433502\ln T$$

$$\ln e_i(T) = -6024.5282\,T^{-1} + 24.7219 + 1.0613868\times10^{-2}\,T - 1.3198825\times10^{-5}\,T^2 - 0.49382577\ln T$$

$e_w(T)$ and $e_i(T)$ in hPa and T in K

The first and second derivatives, $e'_L=de_L/dT$ and $e''_L=d^2e_L/dT^2$ can be computed numerically from these relations.

8. References

1. H. Appleman, *Bull. Amer. Meteor. Soc.*,1953, **34**, 14-20
2. U. Schumann, *Meteorol. Zeit.*, 1996, **5**, 4-23
3. B. Kärcher, *J. Geophys. Res.*, 1995, **100**, 18835-18844
4. B. Kärcher, M.M. Hirschberg and P. Fabian, , *J. Geophys. Res*, 1996, **101**, 15169-15190
5. R. Busen and U. Schumann, *Geophys. Res. Lett* ,1995, **22**, 1357-1360
6. V. Freudenthaler, F. Homberg and H. Jäger, *Geophys. Res. Lett.*, 1995, **22**, 3501-3504
7. K. Sassen, *Bull. Amer. Meteor. Soc*, 1997, **78**,1885-1903
8. U. Schumann and P. Wendling, In: Air Traffic and Environment - Background, Tendencies and Potential Global Atmospheric Effects, U. Schumann (ed.), Springer Verlag, 138-153
9. S. Bakan, M. Betancor, V. Gayler and H. Graβl, *Ann. Geophys.*, 1994, **12**, 962-968
10. T. Gerz, T. Dürbeck and P. Konopka, *J. Geophys. Res.*, submitted
11. H. Mannstein, In: Proceedings of the Impact of Aircraft upon the Atmosphere International Colloqium, 1997, Vol. II, 427-431
12. A. Schmitt and B. Brunner, DLR-Mitt., 1997, 97-40
13. M. Boin and L. Levkov, *Ann. Geophys.*, 1994, **12**, 969-978
14. M. Kästner, K.T. Kriebel, R. Meerkötter, W. Renger, G.H. Ruppersberg and P. Wendling, *Mon. Wea. Rev.*, 1993, **121**, 2708-2717
15. H. Jäger, V. Freudenthaler and F. Homburg, *Atmos Environ.*, 1998, in press
16. D.P. Duda, J.D. Spinhirne, *Geophys. Res. Lett.*, 1996, **23**, 3711-3714
17. J.-F.Gayet, G. Febvre, G. Brogniez, H. Chepfer, W. Renger and P. Wendling, *J. Atmos. Sci*, 1996, **53**, 126-138
18. F. Schröder, J.-F. Gayet, R. Meyer, C. Duroure, B. Strauss and S. Borrmann, Virginia Beach NASA Meeting, 1997
19. K. Gierens, *J. Atmos. Sci.*, 1996, **53**, 3333-3348
20. M. Betancor-Gothe and H. Graβl, *Theor. Appl. Climatol.*, 1993, **48**, 101-113
21. G. Brogniez, J.C. Buriez, V. Giraud, F. Parol and C. Vanbauce, *Mon. Wea. Rev.*, 1995, **123**, 1025-1036
22. V. Freudenthaler, F. Homburg and H. Jäger, *Geophys. Res. Lett.*, 1996, 23, 3715-3718
23. B. Strauss, R. Meerkötter, B. Wissinger, P. Wendling and M. Hess, *Ann. Geophys*, 1997, **15**, 1457-1467
24. J.P.F. Fortuin, R. Van Dorland, W.M.F. Wauben and H. Kelder, *Ann. Geophys.*, 1995, **13**, 413-418

25. P. Minnis, J.K. Ayers and D.R. Doelling, In: Proceedings of the Impact of Aircraft upon the Atmosphere International Colloqium, ONERA, 15-18 Octobre 1996, Paris-Clamart, France, Vol. I, 355-360
26. P.M. Kuhn, *J. Atmos. Sci.*, 1970, **27**, 937-942
27. P. Wendling, R. Büll, M. Kästner, H. Mannstein, F. Schröder and B. Strauss, 1997, Abschlüsbericht zum Forschungsscherpunkt AP1311 des Forschungsverbundes Schadstoffe in der Luftfahrt
28. A.W. Brewer, *Weather*, 1946, **1**, 34-40
29. U. Schumann, J. Ström, R. Busen, R. Baumann, K. Gierens, M. Krautstrunk, F.P. Schröder and J. Stingl, *J. Geophys. Res.*, 1996, **101**, 6853-6869
30. E. J. Jensen, O.B. Toon, S. Kinne, G.W. Sachse, B.E. Anderson, K. R. Chan, C. H. Twohy, B. Gandrud, A. Heymsfield and R. C. Miake-Lye,*J. Geophys. Res.*, 1998, **103**, 3929-3936
31. R. Meerkötter, U. Schumann, P. Minnis, D.R. Doelling, T. Nakajima and Y. Tsushima, to be submitted, 1998
32. P. Minnis, D.F. Young, L. Nuygen, D.P. Garber, W.L. Smith, Jr. And R. Palikonda, *Geophys. Res. Lett.*, 1998, 25, 1157-1160
33. E.J. Jensen and O.B. Toon, *Geophys. Res. Lett.*, 1997,24, 249-252
34. P. Minnis, J.K. Ayers and S.P. Weaver, In: Proceedings of the impact of aircraft upon the atmosphere international colloquium, ONERA, 15-18 October 1996, Paris- Clamart, France, Vol I, 355-360
35. R. Sausen, K. Gierens, M. Ponater and U. Schumann, *Institut für Physik der Atmosphäre*, report No. 89
36. M. Ponater , S. Brinkop, R. Sausen and U. Schumann, In: Proceedings of the impact of aircraft upon the atmosphere international colloquium, ONERA, 15-18 October 1996, Paris- Clamart, France, Vol I, 373-378
37. K.-N. Liou, S.C. Ou and G. Koenig, In: Air Traffic and the Environment: Background, Tendencies, and Potential Glabal Atmospheric Effects, U. Schumann (ed.), Springer-Verlag, New York, pp. 154-169
38. M. Ponater, S. Brinkop, R. Sausen and U. Schumann, *Ann. Geophys.*, 1996, **14**, 941-960
39. D. Sonntag, *Meteorol. Z., N.F.*, 1994, **3**, 51-66
40. K.N. Liou, P. Yang, Y. Takano, K. Sassen, T. Charlok and W. Arnott, *Geophys. Res. Lett.*, 1998, **25**, 1161-1164
41. D.P. Duda, J.D. Spinhirne and W.D. Hart, *Geophys. Res. Lett.*, 1998, **25**, 1149-1152
42. K. Sassen and C. Hsueh, *Geophys. Res. Lett.*, 1998, **25**, 1165-1168
43. H. Mannstein, *Institut für Physik der Atmosphäre*, report No. 92
44. H. Mannstein, R. Meyer and P. Wendling, *Int. J. Remote Sensing.*, submitted

45. J. Travis and S.A. Changnon, *J. Wea. Mod.*, 1997, **29**, 74-83
46. Brockhagen, 1996, quoted in G. Brasseur, European Scientific Assessment of the Atmospheric Effects of Aircraft Emissions, *Atmos. Env.*, in press
47. IPCC (Intergovernmental Panel on Climate Change), 1994
48. B. Kärcher, Th. Peter and R. Ottmann, *Geophys. Res. Lett.*, 1995, **22**, 1501-1504
49. P. Minnis, J.K. Ayers and S.P. Weaver, NASA Reference Publ. 1404
50. J. Diehl and S.K. Mitra, *Atmos. Env.*, 1998, in press
51. U. Schumann, *Ann. Geophys.*, 1994, **12**, 365-384
52. R. P. Lawson, A.J. Heymsfield, S.M. Aulenbach and T.L. Jensen, *Geophys. Res. Lett.*, 1998, **25**, 1331-1334
53. A.J. Heymsfield, R. P. Lawson and G.W. Sachse, *Geophys. Res. Lett.*, 1998, **25**, 1335-1338
54. Q. Fu and K.N. Liou, *J. Atmos. Sci.*, 1993, **50**, 2008-2025
55. G.N. Plass, G.W. Kattawar and F.E. Catchings, *Appl. Opt.*,1973, **12**, 314-329
56. T. Nakajima and M. Tanaka, *J. Quant. Spectrosc. Radiat. Transfer.*, 1986, **35**, 13-21
57. T. Nakajima and M. Tanaka, *J. Quant. Spectrosc. Radiat. Transfer.*, 1988, **40**, 51-69
58. J. Goodman, R.F. Pueshel, E.J. Jensen, S. Verma, G.V. Ferry, S.D. Howard, S.A. Kinne and D. Baumgardner, *Geophys. Res. Lett.*, 1998, **25**, 1327-1330
59. B. Kärcher, R. Busen, A. Petzold, F.P. Schröder, U. Schumann and E.J. Jensen, *Geophys. Res. Lett.*, submitted